

Project 1: System Behaviors and Complexity Measures of FitzHugh-Nagumo Oscillators

JEB 1444H: Neural Engineering

Yichun Zhang

March 10, 2022

Table of Contents

Part I: The Intrinsic Frequency as a Function of Stimulus Intensity	3
Part II: The Neuronal Phase Coherence Map for Coupled Oscillators	4
Part III: The Complexity Measures of the Coupled Oscillators	6
Method	6
1) Embedding Dimension & Time Delay	6
2) Correlation Dimension	6
3) Maximum Lyapunov Exponent	6
Complexity Measure Maps	6
Chaotic Behavior with Specific Frequency and Coupling Strength	10

Part I: The Intrinsic Frequency as a Function of Stimulus Intensity

For the *FitzHugh-Nagumo* oscillator model:

$$\dot{x} = \alpha \left[y + x - \frac{x^3}{3} + z \right]$$

$$\dot{y} = -\frac{1}{\alpha} [\omega^2 x - a + by]$$

where the parameters were taken values $a = 0.7, b = 0.8, \omega^2 = 1, \alpha = 2$, and z is the stimulus intensity of a constant value, the intrinsic frequency of the oscillator output was obtained at varying stimulus intensity using the `ode15s` solver in MATLAB. It was found that periodic oscillations occurred between $z = -0.34$ and $z = -1.40$. Intrinsic frequency as a function of stimulus intensity is illustrated in Figure 1. It can be observed that within the oscillatory range, the intrinsic frequency has a parabolic-like relationship with the stimulus intensity. In details, the intrinsic frequency has lowest value of 0.08 per second at the boundaries $z = -0.33$ and $z = -1.4$, and it reaches its maximum of 0.105 per second at $z = -0.9$.

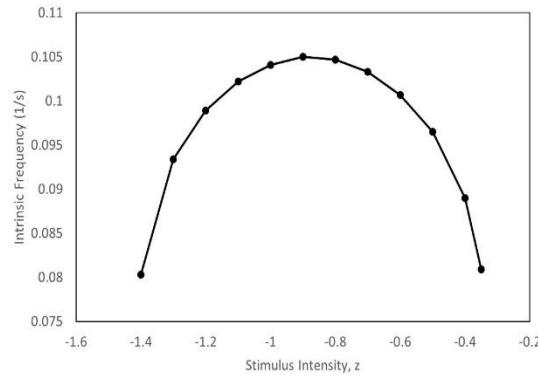


Figure 1. Intrinsic frequency as a function of stimulus intensity

The oscillatory behavior of the system is tested at the two boundaries at shown in Figure 2. Outside this range of stimulus intensity -1.40 to -0.34, the system is damped and converges to a constant rapidly.

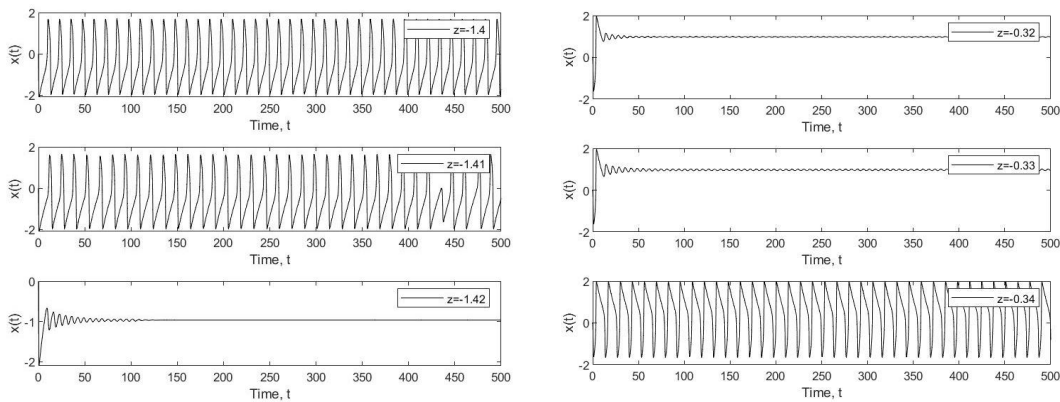


Figure 2. Oscillatory behavior at the boundary stimulus intensity.

Part II: The Neuronal Phase Coherence Map for Coupled Oscillators

When two of the *FitzHugh-Nagumo* oscillators are coupled bidirectionally by a symmetric coupling strength c as expressed below:

$$\begin{aligned}\dot{x}_1 &= \alpha \left[y_1 + x_1 - \frac{x_1^3}{3} + (k_1 + cx_2) \right] \\ \dot{y}_1 &= -\frac{1}{\alpha} [\omega^2 x_1 - a + by_1] \\ \dot{x}_2 &= \alpha \left[y_2 + x_2 - \frac{x_2^3}{3} + (k_2 + cx_1) \right] \\ \dot{y}_2 &= -\frac{1}{\alpha} [\omega^2 x_2 - a + by_2]\end{aligned}$$

k_1 and k_2 are associated with the intrinsic frequency of x_1 and x_2 respectively, thus were estimated using the range of stimulus intensity for oscillatory system as obtained in Part I (i.e., assuming $c = 0$). The oscillator outputs were again solved using the `ode15s` solver in MATLAB. A neuronal phase coherence index R was obtained at different combinations of percentage intrinsic frequency different and symmetric coupling strength using the equation:

$$R = \left| \frac{1}{N} \sum_{j=1}^N e^{i[\phi_{x1}(t_j) - \phi_{x2}(t_j)]} \right|$$

where $\phi_{x1}(t)$ and $\phi_{x2}(t)$ are the phase time series obtained from the imaginary part of the Hilbert Transform of $x_1(t)$ and $x_2(t)$ respectively using function `Hilbert` in MATLAB. The coherence index response map at varying percentage intrinsic frequency difference $(k_1 - k_2)/k_1$ and symmetric coupling strength is illustrated in Figure 2. In Figure 3, the coherence index R is plotted against the coupling strength at a constant percentage intrinsic frequency difference of -0.05.

As shown in Figures 2 and 3, at zero coupling, the coherence index R drops to zero, and it increases rapidly and continuously with increasing positive c . Within the positive c region, R is optimized in a 2D-horn shaped region (shown as bright yellow in Figure 2) with its vertex located near $c = 0^+$ and $\Delta k/k_1 = 0$. Within this region, the oscillators x_1 and x_2 are in perfect synchrony.

In the negative c region, it appears that there is a triangular region (shown as dark blue in Figure 2) where R diminishes from approximately 0.4 to 0 with decreasing c . At the edge of this region, R approaches the minimum from the right and hits a discontinuity point, where R values to the left of this contour are around 0.6 to 0.8, but those to the right of the contour are generally less than 0.3. This discontinuity can also be observed from Figure 4 at the grey dashed line. At this stage, it can be preliminarily predicted that chaotic behaviours are likely to occur along this contour due to the erratic change of coherence between the oscillators.

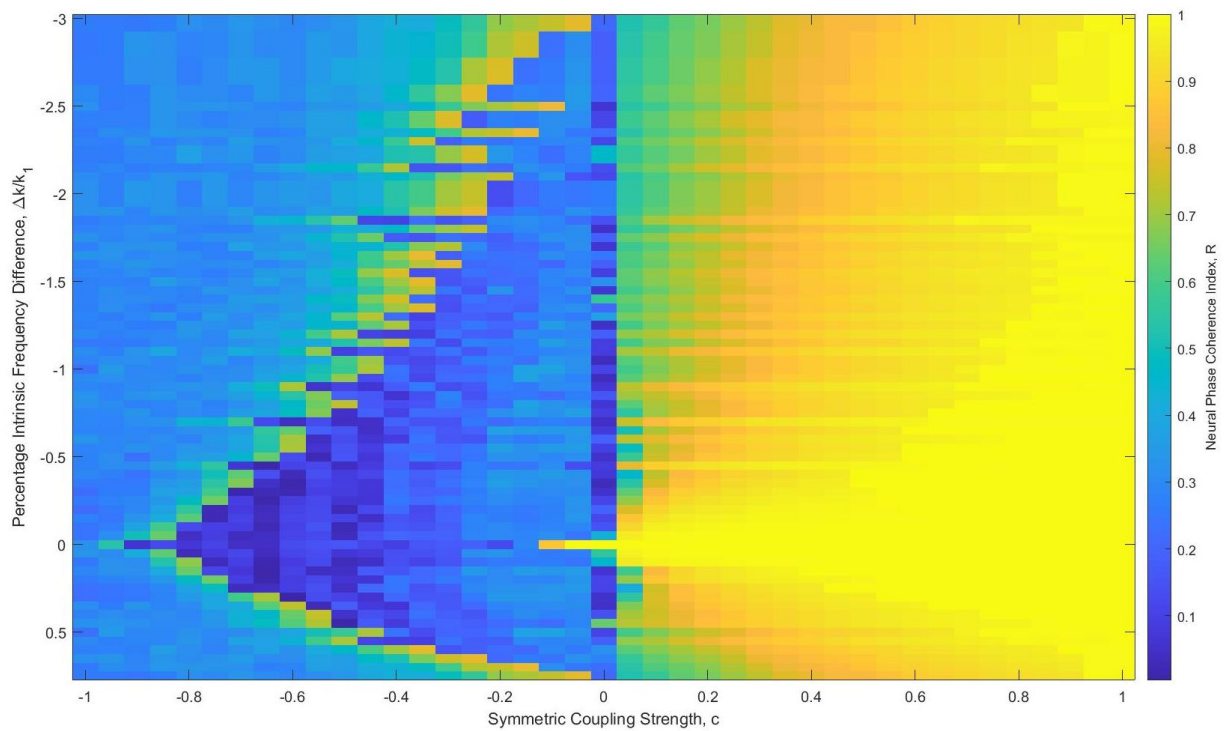


Figure 3. Neuronal phase coherence map at varying percentage intrinsic frequency difference and symmetric coupling strength

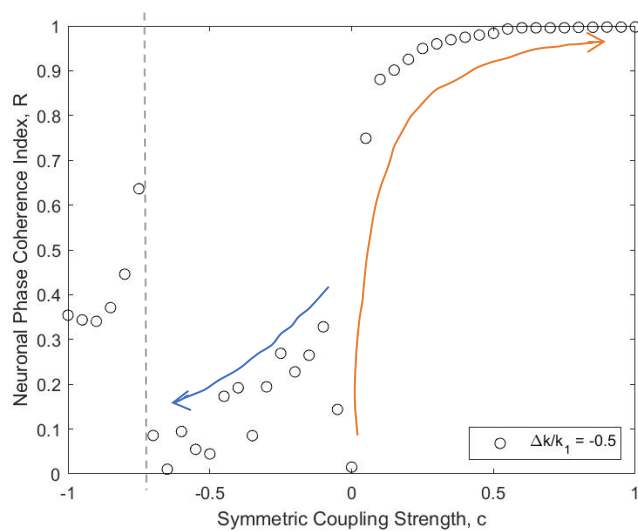


Figure 4. Coherence dependence on coupling strength

Part III: The Complexity Measures of the Coupled Oscillators

Method

1) Embedding Dimension & Time Delay

The embedding dimension and time delay were found by performing the `phaseSpaceReconstruction` function to each point in the time series. In general, the embedding dimensions are taken between 3 and 4 and time delays are taken between 8 and 10 for the following computations.

2) Correlation Dimension

A Grassberger-Procaccia algorithm was used to compute the correlation dimension D_c of each oscillator using the `correlationDimension` function in MATLAB. All D_c values have been calibrated to retain zero D_c at zero symmetric coupling.

3) Maximum Lyapunov Exponent

A Rosenstein's algorithm was used to compute the maximum Lyapunov exponent λ_{\max} of the two oscillatory signals x_1 and x_2 respectively. MATLAB function `lyapunovExponent` was performed with a default sampling frequency of 2π . All λ_{\max} values have been calibrated to retain zero λ_{\max} at zero symmetric coupling.

Complexity Measure Maps

As shown in Figures 5 and 6, x_1 and x_2 have similar correlation dimension maps. The value of D_c ranges from -1.3 to 0.7 with positive values mainly being within the region outlined by red dashed lines, where higher levels of chaotic complexity are expected. In addition, as being agreed by the prediction from the coherence map, the left side boundary of this region have multiple points with a D_c value of as high as 0.4 to 0.7, indicating possible chaotic activity. Outside this region, D_c is uniformly smaller than zero, which implies stable or dissipative system behavior.

In Figures 7 and 8, the same phenomenon can be observed. The λ_{\max} values of x_1 and x_2 range from -0.8 to 0.4, in which the points with higher λ_{\max} are generally located in the same region. This is expected as both high D_c number and high λ_{\max} value are associated with chaotic behavior.

In conclusion of all the computation results at this stage, chaotic behavior is most likely to occur at a point where it is close to the life boundary of the outlined region and has positive D_c or λ_{\max} values for both $x_1(t)$ and $x_2(t)$. Hence, in order to search for chaos more specifically, a grid on the map located at $\Delta k/k_1 = -2.35$ and $c = -0.05$ is selected for further complexity measures (shown in a red circle in Figures 5, 6, 7, and 8).

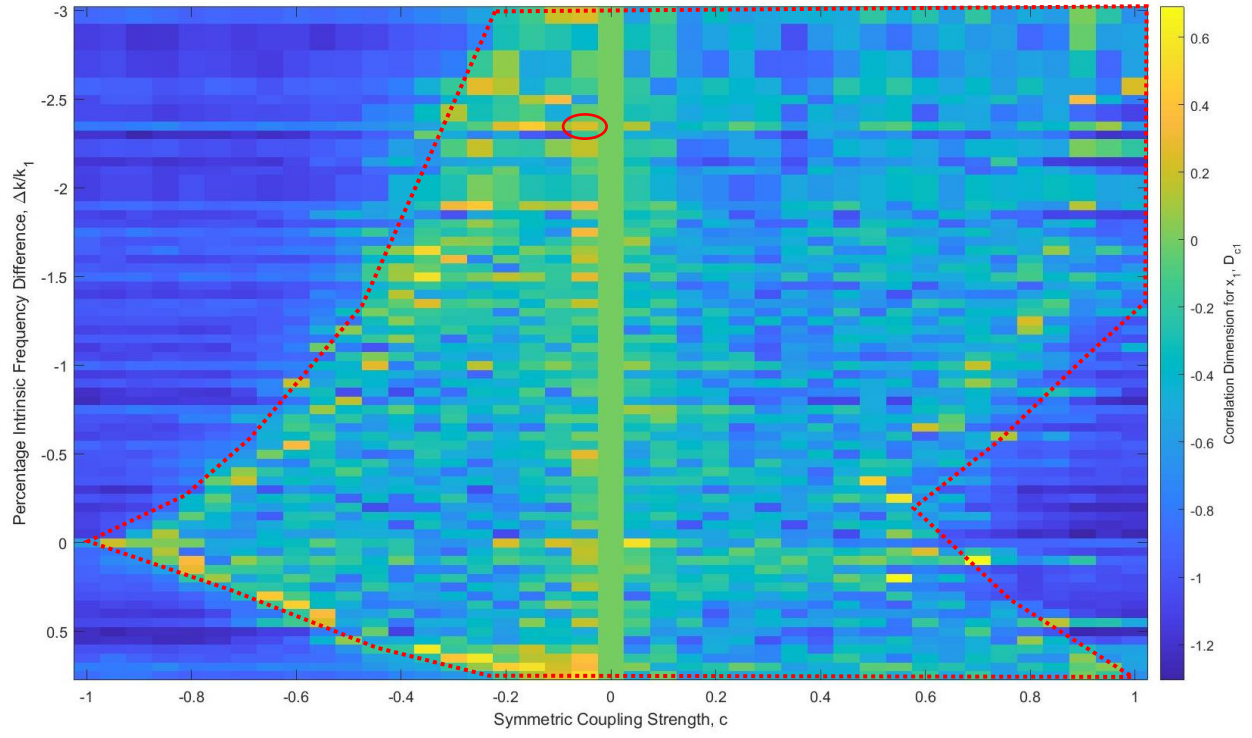


Figure 5. Correlation dimension map for x_1

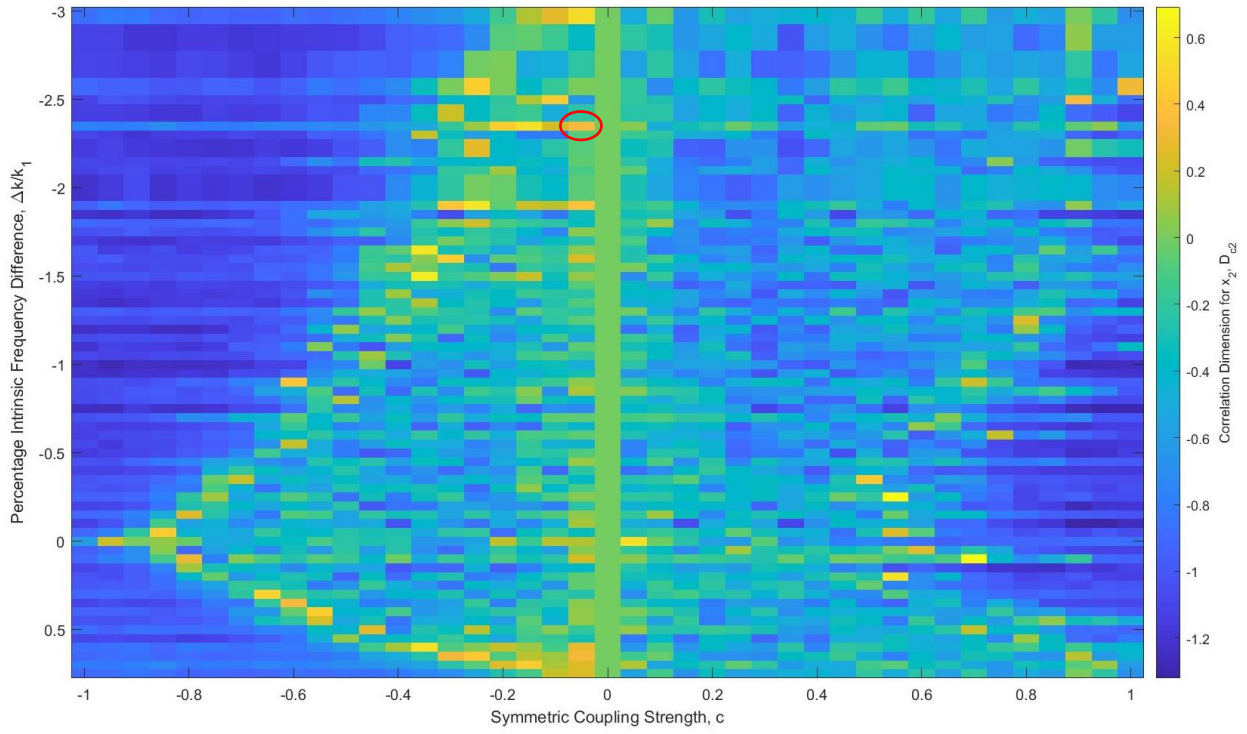


Figure 6. Correlation dimension map for x_2

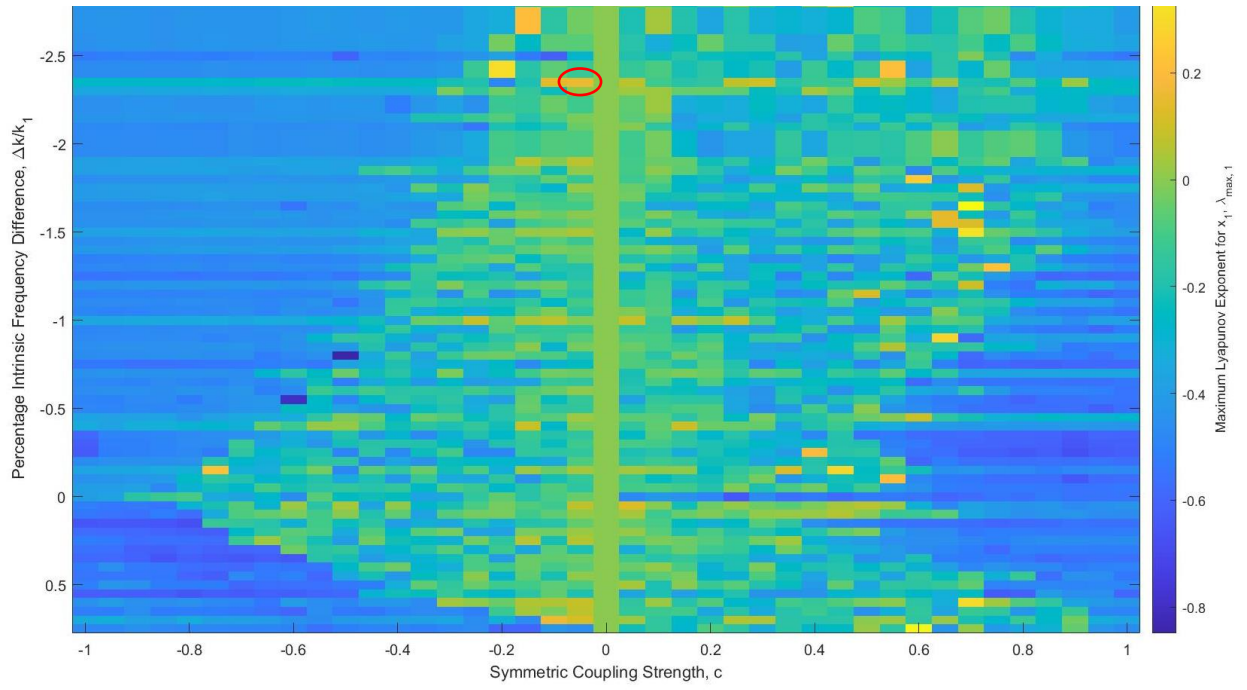


Figure 7. Maximum Lyapunov exponent map for x_1

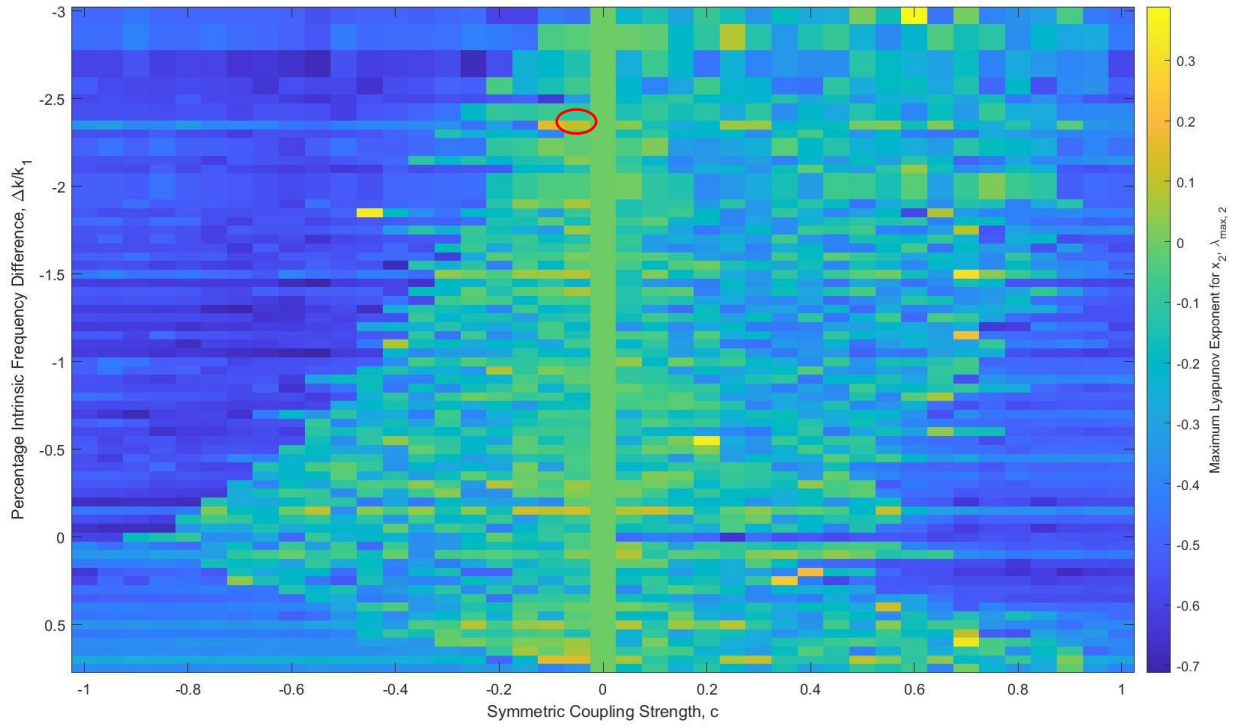


Figure 8. Maximum Lyapunov exponent map for x_2

The sample complexity measure computations were applied to the region $-2.40 \leq \Delta k/k_1 \leq -2.20$ and $-0.1 \leq c \leq 0$ as shown in Figure 9. Again, all data were calibrated with zero complexity at zero coupling.

A similar procedure as described before is repeated. A plot located near $\Delta k/k_1 = -2.23$ and $c = 0.025$ shows positive complexity measures D_c and λ_{\max} in all subplots in Figure 9. Hence, it is believed that chaotic behavior between the interaction of x_1 and x_2 is likely to occur under such condition. This prediction shall be verified when chaotic phase plane and time series are obtained at this point.

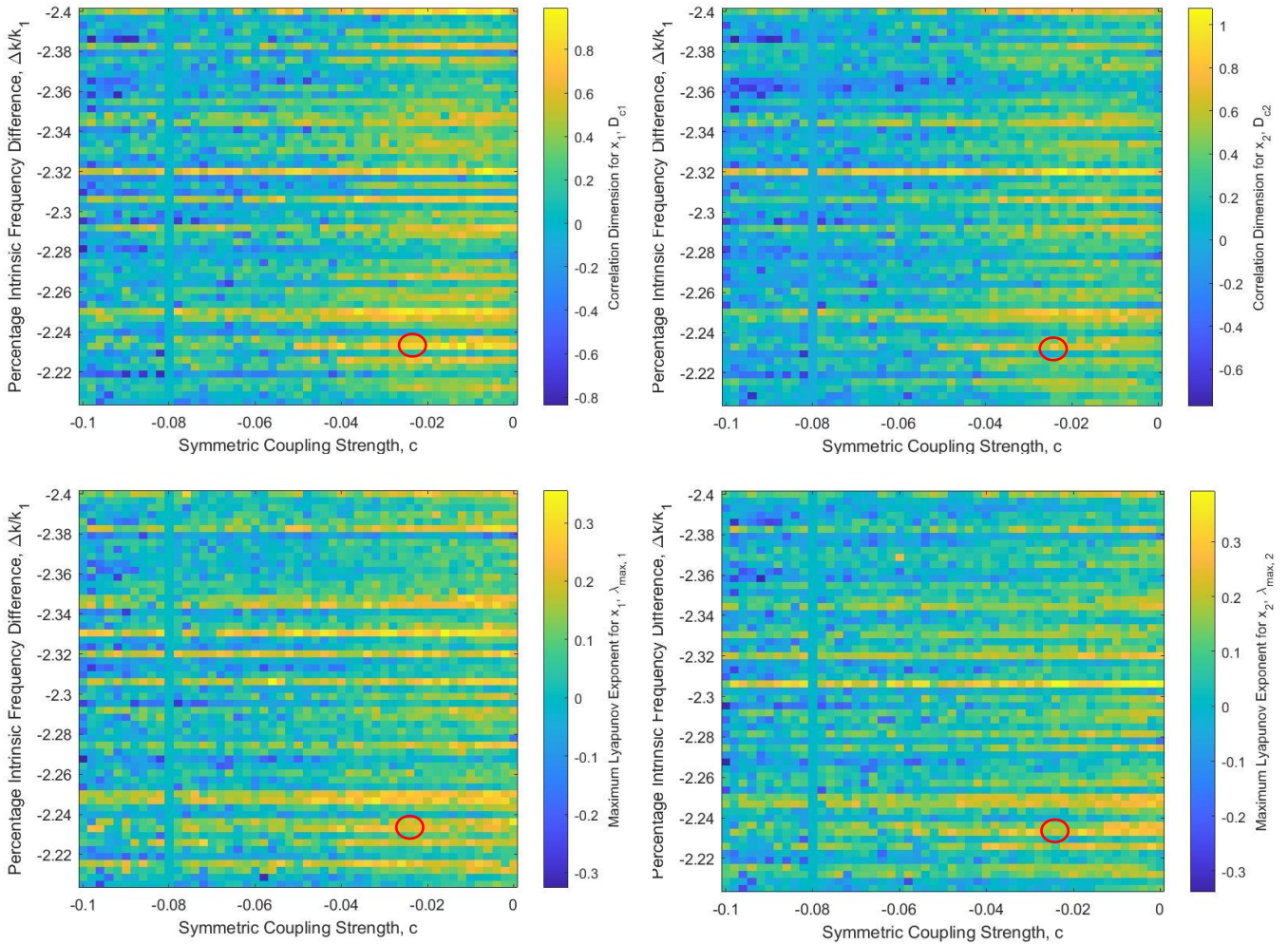


Figure 9. Complexity Measures at $-2.40 \leq \Delta k/k_1 \leq -2.20$ and $-0.1 \leq c \leq 0$

Chaotic Behavior with Specific Frequency and Coupling Strength

The procedure being described in Part II were performed iteratively at different locations on the complexity maps. After repeated searching and complexity calculations, chaotic behaviors were found at the following conditions:

$$1) \Delta k/k_1 = 0.7156, \quad c = 0.0143$$

$$2) \Delta k/k_1 = -2.217, \quad c = -0.024$$

The time series of $x_1(t)$ and $x_2(t)$ as well as their interactive phase plane at these conditions are shown in Figures 10 and 11 respectively. In the 1st case, $x_2(t)$ shows chaotic behavior, resulting in irregular activity in the phase plan. Whereas, in the 2nd case, $x_1(t)$ is chaotic instead.

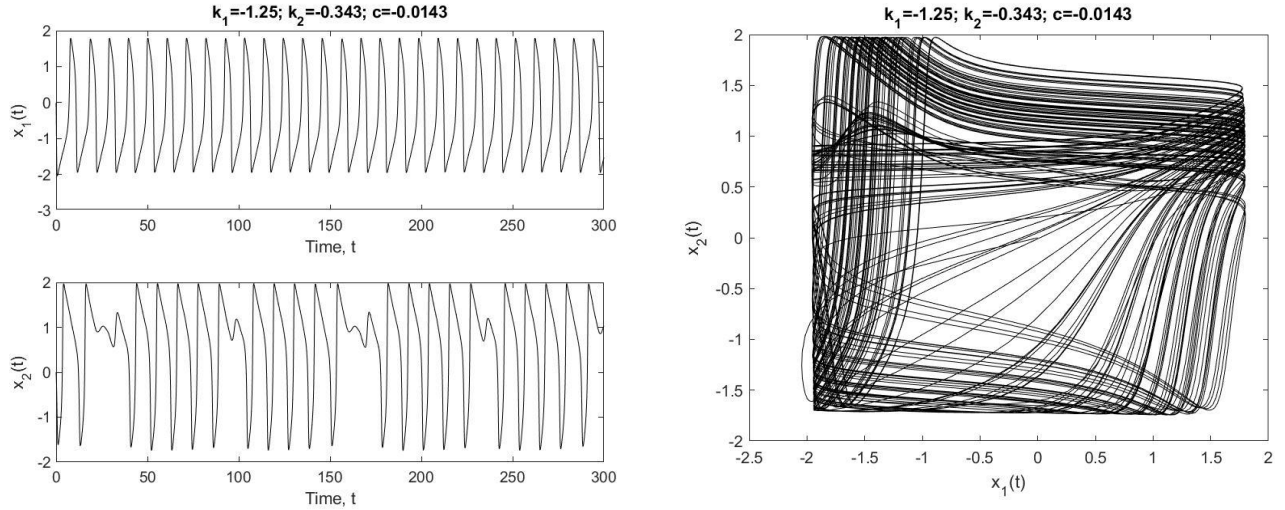


Figure 20. Time series and phase plane when $\Delta k/k_1 = 0.7156$, $c = 0.0143$

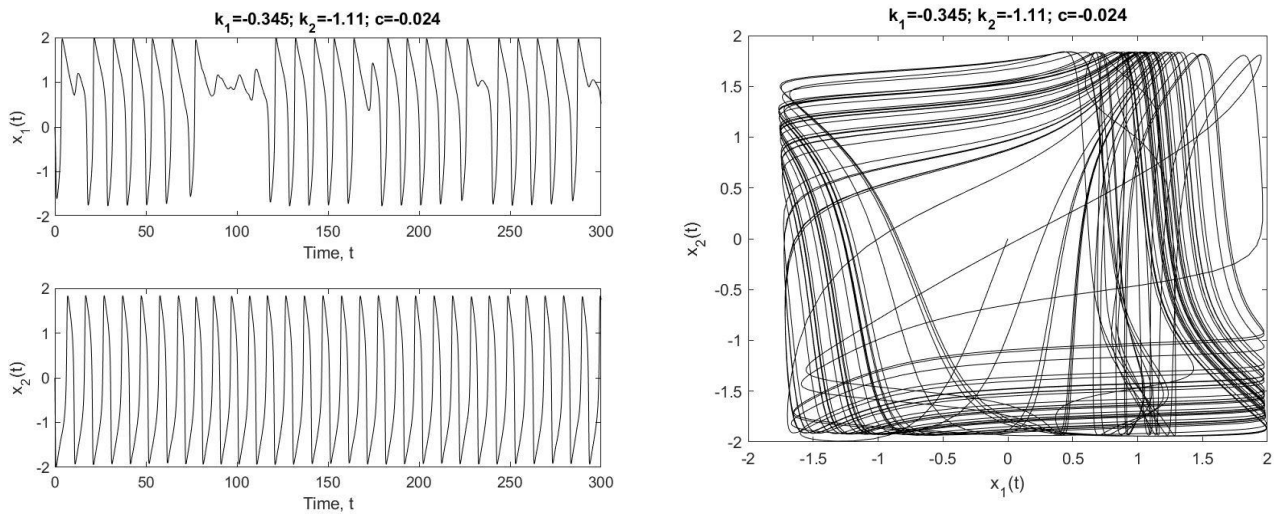


Figure 11. Time series and phase plane when $\Delta k/k_1 = -2.217$, $c = -0.024$

Finally, it is expected that there are other combinations of $\Delta k/k_1$ and c that could result in chaotic oscillatory output. However, due to the limitations of the numerical computation and time constraint, only the two conditions being illustrated above is included in the scope of this study. More awaits to be explored.